PERGAMON

Neuropsychologia 41 (2003) 1817–1836

NEUROPSYCHOLOGIA

www.elsevier.com/locate/neuropsychologia

Can spatial and temporal motion integration compensate for deficits in local motion mechanisms?

Lucia M. Vaina [a,b,*], Norberto M. Gryzwacz [c], Pairash Saiviroonporn [a,b], Marjorie LeMay [b], Don C. Bienfang [b], Alan Cowey [d]

[a] *Brain and Vision Research Laboratory, Biomedical Engineering and Neurology, Boston University, Boston, MA, USA*
[b] *Departments of Neurology, Ophthalmology and Radiology, Harvard Medical School, Boston, MA, USA*
[c] *Department of Biomedical Engineering and Neuroscience Graduate Program, University of Southern California, University Park, OHE 500, 3650 S. McClintock Avenue, Los Angeles, CA 90089-1451, USA*
[d] *Department of Experimental Psychology, University of Oxford, South Parks Road, Oxford OX1 3UD, UK*

Received 24 April 2003; accepted 20 June 2003

Abstract

We studied the motion perception of a patient, AMG, who had a lesion in the left occipital lobe centered on visual areas V3 and V3A, with involvement of underlying white matter. As shown by a variety of psychophysical tests involving her perception of motion, the patient was impaired at motion discriminations that involved the detection of small displacements of random-dot displays, including local speed discrimination. However, she was unimpaired on tests that required spatial and temporal integration of moving displays, such as motion coherence. The results indicate that she had a specific impairment of the computation of local but not global motion and that she could not integrate motion information across different spatial scales. Such a specific impairment has not been reported before.

Keywords: Motion perception; D-Max; Local motion; Global motion; Extra-striate cortex

1. Introduction

Velocity is the temporal derivative of distance. Its measurement should therefore be localized in space and time. Unsurprisingly, visual neurons are well suited to estimate motion parameters in a relatively localized manner. For instance, in macaque monkeys directionally selective neurons in cortical area V1 with foveal receptive fields perform their computations in less than about 100 ms and across about 30 arcmin (Mikami, Newsome, & Wurtz, 1986a,b). With random-dot kinematograms (RDKs) this is reflected perceptually in human vision as the overall direction of the jumps of the dots. The direction can only be detected reliably over a limited distance of around 15–30 arcmin with an inter-frame interval of less than 80 ms (Braddick, 1974). This is the maximum spatial displacement within which this type of motion discrimination is possible, and is referred to as D-Max. The mechanism mediating this perception was called by Braddick, 1974 "short-range" process, and supposedly it corresponds to low-level motion. Psychophysical studies suggested (Braddick, 1974; Baker & Braddick, 1982; Nakayama & Silverman, 1984; Sato, 1989) that D-Max in RDK displays is limited by absolute visual angle not by the number of dots, and this motivated his proposal that D-Max in RDKs is determined by the receptive field size and not by higher level processes such as feature correlation. Accordingly models of low-level early motion detection (Reichardt, 1965, 1987; Adelson & Bergen, 1985; Van Santen & Sperling, 1985; Watson & Ahumada, 1985) adopted these spatial and temporal constraints in their parameters.

As well as motion direction, speed seems to be estimated locally. The smallest speed difference that experienced subjects can reliably detect, presented as the Weber fraction ($\Delta V/V$) is roughly 0.05, whether the moving stimuli are dot fields, lines, or sinusoidal gratings (McKee, 1981; McKee, Silverman, & Nakayama, 1986; Bravo & Watamaniuk, 1995; De Bruyn & Orban, 1988; Pasternak, 1987; Watamaniuk & Duchon, 1992). Furthermore, the perceptual segregation of two overlapping random-dot cinematograms moving in the same direction but with different speeds (motion transparency) relies on the computation of local speed signals. Such psychophysical findings have inspired the development of models for computing local velocity (Watson & Ahumada, 1985; Heeger, 1987; Heeger, Simonceli & Movshon, 1995; Grzywacz & Yuille, 1990; Heeger & Simoncelli, 1992).

* Corresponding author. Fax: +1-617-353-6766.
E-mail address: vaina@engc.bu.edu (L.M. Vaina).

0028-3932/$ – see front matter © 2003 Published by Elsevier Ltd.
doi:10.1016/S0028-3932(03)00183-0

The models all emphasize the integration of the responses of directionally selective neurons tuned to different spatial and temporal frequencies across the extent of their receptive field. They constrain the velocity calculation to use only local information, thus reducing the probability that the motion of different objects is combined in the velocity estimate.

Even the computation of motion parameters for more complex stimuli such as plaids formed by two overlapping sinewave gratings moving in different directions may be partly localized (Adelson & Movshon, 1982). Plaids are perceived as moving rigidly, i.e. in one direction, when the properties of the composing grating are similar, but otherwise the percept is two gratings sliding across each other. The neural substrates of these rigid and transparent perceptions were suggested to be the so-called pattern and component cells, respectively in area MT (Rodman & Albright, 1989). It was proposed (Adelson & Movshon, 1982) that the computation of a plaid's rigid motion was performed in two stages: (1) extraction of information on motion perpendicular to the orientation of the grating (performed by component cells); and (2) computation of the intersection of all motions consistent with the grating's motion (performed by pattern cells). In advancing this hypothesis, they took into consideration the "aperture problem" (Adelson & Movshon, 1982; Marr & Ullman, 1981; Hildreth, 1984a; Hildreth, 1984b; Hildreth & Koch, 1987), i.e. that in regions of the image where the motion variation is mostly along one dimension (i.e. contour) local mechanisms can only measure motion perpendicular to the contour. Thus, direction selective neurons in V1, with small receptive fields, are assumed to make such ambiguous motion measurements. In contrast, Adelson & Movshon (1982) suggested that component cells can compute local motion correctly. Additionally, they implied that the second stage of their formulation called the "intersection of constraints" (IOC), is a spatially distributed computation which is mediated by the "pattern-motion" selective neurons (Movshon, Addelson, & Gizzi, 1983) in area MT of the primate brain. Such neurons derive the true velocity vector by integrating motion information from several locations on the same moving object.

On computational grounds, Grzywacz and Yuille subsequently argued that neurons in V1 do not suffer, strictly speaking, from the aperture problem, since more than just the orientation component of the stimulus is usually available within their receptive fields (Grzywacz & Yuille, 1990; Grzywacz, Smith, & Yuille, 1989). They emphasized instead that the problem facing these cells is their inability to compute local velocity correctly. Not only are they not tuned to a unique speed, but also, depending on the stimulus, may report the "wrong" direction of motion. They accordingly suggested a three-stage model of visual-motion computation consisting of: (1) extraction of local directional information, necessarily confounded by spatio-temporal frequencies and contrast; (2) extraction of an unconfounded local velocity signal (where rigid-plaid motion would already be computed); and (3) spatio-temporal integration of local velocity signals. The integration solves the true aperture problem, improves the signal-to-noise ratio, and encodes complex motion patterns such as a rotation, expansion, and shear. There is independent psychophysical evidence (Ferrera & Wilson, 1990; Yo & Wilson, 1992) for the hypothesis that the human visual system does not implement the IOC construction in specific details.

The above considerations highlight the fact that although the early computation of motion is relatively local, global mechanisms of spatial and temporal integration contribute to the final percept. Psychophysical studies demonstrated that human observers can detect signals extended in the direction of motion more accurately than is expected from low-level motion detectors (Anstis & Ramachandran, 1987; Snowden & Braddick, 1989; Verghese, Watamaniuk, McKee, & Cryzywacz, 1999). Evidence for the role of temporal integration was provided by Nakayama and Silverman (1984) who showed that D-Max increases if the judgement of the jump is preceded by motion in the direction of the jump ("temporal recruiting"). Moreover, speed discrimination improves with the duration of the motion and the visual system uses the immediately preceding motion to disambiguate visual displays that would otherwise be ambiguous. A computational model to account for such temporal integration effects has been suggested (Grzywacz, Smith, & Yuille, 1989).

Spatial integration of motion signals is apparent at the neurophysiological level in neurons (in area MT, for example) whose receptive fields are larger than those of their V1 inputs by as much as a factor of 10 (Maunsell & Van Essen, 1983; Movshon & Newsome, 1996; Tanaka, Hikosake, Saito, Yukie, Fududa & Iwaia, 1986) and therefore are good candidates to perform spatial summation of their input motion information. Thus several studies have suggested that MT neurons average multiple inputs of local motions to extract a global direction (Yo & Wilson, 1992; Newsome & Paré, 1986; Newsome & Wurtz, 1988; Newsome, Britten, Salzman, & Movshon, 1990; Snowden, Treue, Erickson, & Andersen, 1991) Furthermore, the responses of individual neurons in area MT of monkeys correlate well with the ability of the animal to solve tasks that require spatial integration of noisy motion signals (Britten, 1993; Newsome, Britten, & Movshon, 1989; Salzman, Britten, & Newsome, 1990). Unilateral lesions of MT of the macaque significantly impair the coherence thresholds in the contralesional visual field, that is the proportion of coherently moving dots (signal) necessary to reliably discriminate the global direction of stimulus motion (Newsome & Paré, 1988). Similar deficits were shown in human patients with lesions involving MT (Baker, Hess, & Zihl, 1990; Vaina, Lemay, Bienfang, Choi, & Nakayama, 1990; Vaina, 1994, 1998). Braddick (1993) argued that spatial integration is particularly important for smoothing noise or sparse motion signals. Spatial integration of motion was also recognized as an important perceptual mechanism by the Gestalt school of psychology, as exemplified by the concept of "common fate". More recent studies have investigated the contribution of spatial

integration to motion perception through phenomena like "motion capture" or "motion cooperativity" (Williams & Brannan, 1994; Nawrot & Sekuler, 1990).

The relationship between local and global computations of motion is relevant to many motion tasks. An important example addressed in this paper is the computation of image discontinuities solely from motion cues. Almost by definition, discontinuities imply a local computation as they require an infinite spatial derivative of some visual quantity such as direction of motion or speed. However, a class of popular models of motion discontinuities based on Markov random fields and line processors requires that separate discontinuities be computed at the same stage of analysis and simultaneously with the spatial integration of motion signals (Koch, Wang, & Mathur, 1989). Our own psychophysical studies of patients with selective motion deficits (Vaina, Grzywacz, & Kikinis, 1994; Vaina, Grzywacz, LeMay, Bienfang, & Wolpow, 1998) have challenged these models. For example, we demonstrated a double dissociation of deficits: patients selectively impaired in computing motion discontinuity without an impairment in spatial integration, and other patients whose discontinuity perception is normal despite an impairment in the extraction of discontinuity from motion. The latter finding, however, does not rule out the possibility that discontinuities and integration are computed separately, but that they interact. Such interaction, for example, would be useful for the computation of discontinuities in noisy images.

In this paper, we describe psychophysical evaluations of local and global computations of motion in patient AMG who, after a cerebrovascular accident (stroke) in the posterior portion of the left hemisphere, presented with deficits on some, but not all, motion tasks. On tests of spatio-temporal filtering at the postreceptoral level, her contrast sensitivity for sinusoidal gratings was impaired for speed discrimination, but not for the discrimination of direction or orientation or for various detection tasks of static or moving gratings. This initially surprising selective deficit for speed suggested that some of her local motion mechanisms might be impaired. We therefore conducted a psychophysical study of her perceptual abilities on five motion-related issues: First, we studied whether her D-Max was smaller than normal and, therefore, the nature of the role of temporal integration mechanisms on D-Max. Second, since a deficit on D-Max often suggests a deficit of local speed discrimination, we investigated the possible impairment of local speed discrimination and the role of temporal integration. We found that AMG was impaired on local speed discrimination, and thus our third line of inquiry probed whether local speed impairment resulted from an impairment in spatio-temporal frequency (TF) mechanisms. Fourth, we studied the relationship between the local and global (more integrative) mechanisms by assessing her ability to perceive motion of rigid-plaids and her perception of spatially coherent global motion. Fifth, we investigated whether the computation of motion discontinuities relies only on local motion information.

2. Methods

2.1. Subjects and general experimental procedures

The subjects were graduate students, the patient AMG and 22 subjects age-matched to the patient, ±3 years. All subjects were naive to the purpose of the experiments and had no prior experience with psychophysical testing. All were right-handed, like AMG. The number of control subjects varied across experiments; where the number was below 16 they were all age-matched to AMG. All subjects (including AMG) had normal or corrected-to-normal visual acuity. Those who required corrective lenses always wore them. Experimental sessions lasted for about 50 min with a 5 min break after each 15 min of testing. All psychophysical tasks were conducted in a darkened room where the chief source of illumination came from the display. The subjects were first familiarized with the display and task, through examples and feedback, and became adapted to the dim illumination. No feedback was provided during the data collection sessions.

The subjects sat without head restraint and viewed the display binocularly from a distance of 60 cm, which was well within their accommodation range. The height of the center of the display (the RGB Monitor or the CRT) was approximately at eye level. In all the experiments the subjects were required to maintain fixation during each trial on a small 4 arcmin × 4 arcmin dark fixation mark placed 2° to the right or to the left of the lateral edge of the viewing aperture. Fixation was monitored informally by the examiner and the few trials in which the subject moved his/her eyes were discarded and repeated. This proved to be straightforward as the examiner had a clear and close-up view of the eyes. Moreover (see below) there was no ophthalmological evidence of unreliable fixation by AMG at the time of testing.

2.2. The patient: neurological, neuroradiological, neuropsychological and neuro-opthalmological examinations

At the time of this investigation the patient, AMG, was a 53-year-old right-handed previously healthy woman who worked as a psychiatric nurse until she sustained an acute left hemisphere haemorrhagic cerebrovascular accident confirmed by computer tomography (CT). The CT scan obtained in the acute care hospital showed an area of hemorrhage in the posterior left hemisphere involving both cortical and white matter tissue. The lesion was postero-lateral to the upper portion of the body of the lateral ventricle and extended up to the surface of the brain in the occipital-parietal region. An angiogram performed a few days later was unremarkable and showed no evidence of AV malformation or vasculitis. Haematologic tests revealed no evidence of bleeding disorder. Magnetic resonance imaging (MRI) a week later revealed a haematoma in the posterior parietal lobe, with the lesion extending downward into the posterior-medial part of

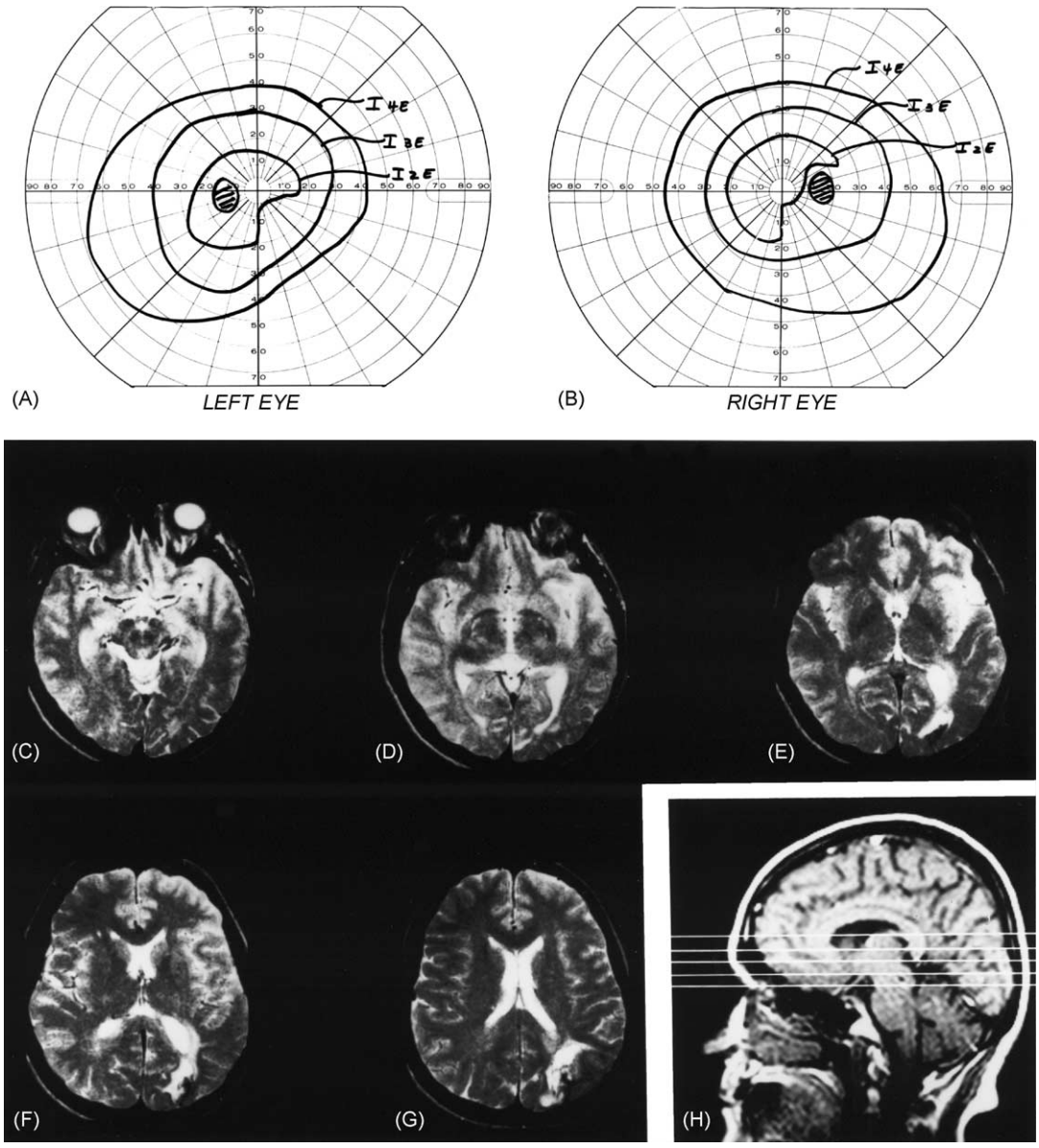

Fig. 1. Visual fields of AMG and axial MR slices illustrating the lesion. A and B show visual fields obtained by Goldmann perimetry, indicating a right inferior quadrantanopia to small targets. Below, C–G illustrate MR axial slices of the brain obtained with a Magnetom 1.5 T unit (6 mm thick slices with 1.2 mm gap). H illustrates a saggital view of the levels of the slices shown (from C the lowest to G the highest). The lesion is not yet seen in C. D: The lesion first appears, at the level of the left lateral ventricle; E: the lesion extends laterally by the margin of the occipital horn of the lateral ventricle to the lateral portion of the occipital lobe and involves slightly the posterior portions of the parietal and temporal lobes. F and G are contiguous slices illustrating the progression of the lesion within the same areas as described in E and showing that the lesion involves primarily the white matter.

the temporal lobe into the central and lateral portion of the occipital lobe but sparing the primary visual cortex (Fig. 1). The lesion extended into the white matter by the trigone of the lateral ventricle and around the margin of the body of the lateral ventricle.

After her stroke AMG remarked that she was unable to carry out normal activities, was bumping into things, and was “reaching in the wrong direction”. Neurological examination in the acute phase, revealed that she had right upper extremity weakness and poor coordination. She had difficulty in following two step commands, was unable to subtract serial seven’s (e.g. given 100 and take away 7, she said 97), and failed the simplest numerical calculations. She could not read numbers but could read letters and words. She made many spelling errors but could write. When asked to spell a word aloud, she could do so correctly. She had no word finding difficulties, except naming numbers. She also had impaired finger naming and a mild limb apraxia for her right hand. Sensory examination and graphesthesia testing revealed extinction on the right to double stimulation. General intellectual function and motor functions were well preserved. On neuropsychological evaluation, on the Wechsler

Memory Scale-Revised (WAIS-R) her verbal I.Q. (VIQ = 96) was in the average range, the Performance I.Q. was in the low average range (PIQ = 80), and the full scale I.Q. in the low average range (FIQ = 88). There was a conspicuous difference between her verbal and perceptual organizational skills, the latter being significantly impaired for her age and educational background, This was not attributable simply to motor slowness. Visual-spatial scanning for target stimuli was normal both from left to right and from right to left (she obtained the maximum score of 30/30). On the Benton line orientation test she scored in the average range (25/30). Two-dimensional form-matching and discrimination were also normal. In contrast, she showed mild deficits on visual-spatial and organizational skills on a task in which she was asked to recognize complex objects that were cut up and would be put together based on features of the objects (Hooper test: score 21.5/30). She tended to be pulled to details of the stimuli. Her performance on the Benton face recognition test was normal.

Snellen acuity was 20/20 in both eyes and visual fields by Goldmann perimetry revealed a right homonymous hemianopia. She had a very slight lateral point nystagmus. A second neurological examination 3 months later showed full recovery from all the deficits noted above. Although on Goldmann perimetry she now had only a right inferior quadrantanopsia it was only for very small targets (2E stimuli, Fig. 1). The nystagmus was now negligible and had disappeared by the time the present results were obtained after a further 2 years.

2.3. Psychophysical assessment

2.3.1. Apparatus and experimental methods

A Macintosh Quadra 700 was used for stimulus generation and data acquisition of the background psychophysical tasks (except the stereopsis and the counterphase flicker tests). The stimuli were displayed on the Apple gray level monitor. A Pelli attenuator was used in connection with the contrast sensitivity test since here it was necessary to achieve low contrast displays. The counterphase flicker stimuli were generated by the Innisfree Picasso image generator (Innisfree, Cambridge, MA) and were displayed on a Hewlett-Packard 1332A CRT equipped with P31 phosphor and at a framerate of 94 Hz. The voltage/luminance relationship was linearized independently for each of the three guns in the RGB display and for the oscilloscope.

The same equipment was used in the psychophysical experimental conditions. The stimuli in Experiments 3 and 7 were sinusoidal gratings generated by the Innisfree Picasso image generator. The stimuli in Experiments 1, 2, 4–6, and 8 were generated by the Macintosh Quadra 700 and were displayed on the Macintosh RGB color monitor (640 × 480 pixels, 8 bit/pixel, with P4 phosphor and 66.7 Hz frame rate). Contrast and luminance measurements of the stimuli in all the displays were performed with a Photo Research Spotometer PR 1510.

Except in Experiment 3 a single-interval forced-choice procedure was used. The responses were entered by the examiner by pressing designated keys on the keyboard. In all the experiments the computer sounded a tone to signal the next trial, after which the fixation mark was displayed, followed by the stimulus. The inter-trial interval was approximately 2 s. Stimuli were displayed either by an adaptive staircase procedure or by the method of constant stimuli (Experiment 7). The steps in the staircase were 1/16th of a log unit. Initially, the staircase went three steps down after each correct answer until the first error occurred. After the first error, the first reversal occurred and the staircase went nine steps up until the second reversal occurred. After the second reversal, the staircase went two steps down for each correct answer until an error occurred and then it went six steps up until the next reversal. After the fourth reversal, the level of difficulty of the stimli increased by a 1/32 of a log unit after three consecutive correct responses, and it decreased by 1/32 of a log unit for each incorrect response. The test ended after 12 reversals and the threshold was calculated as the average of the final six reversals. Each data point plotted for AMG was obtained in at least two independent evaluations, and represents the average and standard deviation of the results of these evaluations. The results from the young and the age-matched normal observers were pooled when there was no clear difference between them.

2.4. Background psychophysical examinations

Three months after the stroke AMG had recovered from most of her initial deficits but she continued to complain that “almost I don’t see any difference in how things move”. This problem interfered with many of her daily activities and prevented her from driving a car. She felt uneasy when walking on the street among many people, remarking that she had “an eerie feeling that I’ll bump into them”. It was difficult for her to cross the street because she felt that she could not appreciate the speed of approaching vehicles. In order to asses her visual capabilities and to evaluate her complaint about perception of motion, she enrolled in our visual-motion perception program. The patient and control subjects gave Informed Consent according to the requirements of the Boston University Human Subjects’ Committee.

We carried out three detailed evaluations of her visual-motion perception abilities at yearly intervals. Her performance on the tests repeated in these evaluations was essentially unchanged (there was no statistically significant difference between the various performances). Every time she was tested, both across years and across days or weeks when different tests were used, she was first tested on the motion coherence task (see Experiment 6) as a baseline. This provided a check on her attentiveness and motivation. She was never impaired on this task. The data presented here are from her most recent evaluation, i.e. about 2.5 years after her stroke.

Spatial contrast sensitivity functions for static and moving sinusoidal gratings and contrast sensitivity as a function of temporal frequency were normal for stimuli presented in either visual field, as was contrast sensitivity for the discrimination of up–down direction of motion, orientation discrimination at contrast threshold (Fig. 2), and temporal frequency discrimination. However, her contrast sensitivity for speed discrimination was impaired for stimuli presented in her right visual field (Fig. 2D). On full field uniform flicker discrimination, in which the task is a cross-comparison of the temporal frequency filters, AMG's performance was normal (comparison with age-matched controls was not statistically significant: $t = 0.96$, $0.2 < P < 0.5$). On the counterphase flicker discrimination task (Fig. 3), which is a cross-comparison of spatial and temporal frequency in a non-directional speed task AMG was impaired for stimuli at temporal frequencies of 10 Hz presented in the right visual field, contralateral to her lesion. The maximum difference between her performance on stimuli in the right and left visual field was at 20 Hz ($t = 3.75$, $P < 0.001$).

Identification of static two-dimensional form (Efron Shapes test) was normal in both visual fields (Fig. 4A). She was severely impaired in both visual fields on discrimination of simple two-dimensional geometric forms defined solely either by speed (Fig. 4C) or direction (Fig. 4D) differences from a dense random-dot pattern which formed the background. Spatial localization abilities were assessed using stimuli consisting of a circle with added 1–4 Gaussian bumps to its circumference. Two-temporal alternatives were used and subjects were asked to report whether the two stimuli were the same. The only variable parameter was the location of one of the bumps in one of the two presentations. AMG's performance was normal for stimuli presented in the left visual field, but she was impaired with stimuli presented in her right visual field (Fig. 4B).

2.5. Stereopsis

We were interested to see whether AMG's ability to detect disparity was different in the two hemifields. The stimuli were computer-generated and viewed through stereoglasses. The test was a 2AFC task in which the subject was asked to make a judgement of whether the binocular target flashed in the center of the screen was in front or behind a reference monocular yellow square displayed in the middle of the screen. The binocular and monocular stimuli each subtended 18 min^2. The subject was asked to maintain fixation on the red arrow. A staircase procedure was used to manipulate disparity values of the target.

Two fixation conditions were presented, one with the fixation mark presented 2° from the target and the other with fixation mark presented 4° from the target. The data from the patient and two normal controls (one experienced and the other naive) show that when the stimuli were presented in the right visual hemifield AMG's threshold was significantly higher, by a factor of about two times in both fixation conditions. The thresholds in the intact left hemifield were non-significantly elevated as compared with the controls. However, most striking was the difference between the patient's results for stimuli presented in the right hemifield, where she was severely impaired compared with the aged matched normal controls for stimuli presented at eccentricities of 2 and 4° (Fig. 5A and B).

2.6. Color perception

The ability to discriminate color was evaluated with the Farnsworth–Munsell test. This test has 88 hues in four groups of 22. A group of 22 is presented in random but predetermined order in a single row. The task is to sort them so that there is an orderly progression of hues along the row between a predetermined anchor hue at each end. AMG's performance on this task was normal. She also scored at a normal level on a task of discrimination of neutral gray values. This is a standard scale of neutral grays (Munsell Color Corp., 1987) ranging between absolute black (0% reflectance) and absolute white (100% reflectance) in steps that look equal to the eye in standard viewing conditions.[1]

2.7. Psychophysical evaluation of motion: local and global motion perception

In experiments using sparse random-dot kinematograms, the display was composed of dots (2 min arc in width) moving at 3°/s. This speed was determined by the ratio of the spatial and temporal offsets, $\Delta t/\Delta x$, and Δt was fixed at 45 ms, which is optimal for psychophysical experiments with humans and monkeys (Movshon, Addelson, & Gizzi, 1983). Each trial consisted of 22 consecutive frames lasting a total of 1 s. A "wrap-around" scheme was used whereby dots displaced beyond the boundary of the aperture reappeared on the opposite side in the next frame. Dot density in dynamic random-dot cinematogram displays (except in Experiments 1 and 4) was 2 dot/degree^2. The background of the display was black and the dots were white. In Experiments 1 and 4 we used denser (50% white and 50 black dots) displays. Further details of these displays are presented in the test description. The second type of dynamic stimuli were simple sinusoidal gratings (Experiment 3) or two superimposed sinusoidal gratings (Experiment 7), details of which are given in the test description.

2.8. Local motion measurements

AMG's contrast sensitivity for speed discrimination was impaired and, because speed appears to involve a local

[1] The Munsell Neutral Values test is presented as 31 matt patches of paper 5° × 5° whose reflectance differed by maximum 6%. The patches were viewed through an oblong white mask with an aperture of 2° × 3° which provided a constant matt background. The task was to sequence the patches of gray in order, from the most white to the most black.

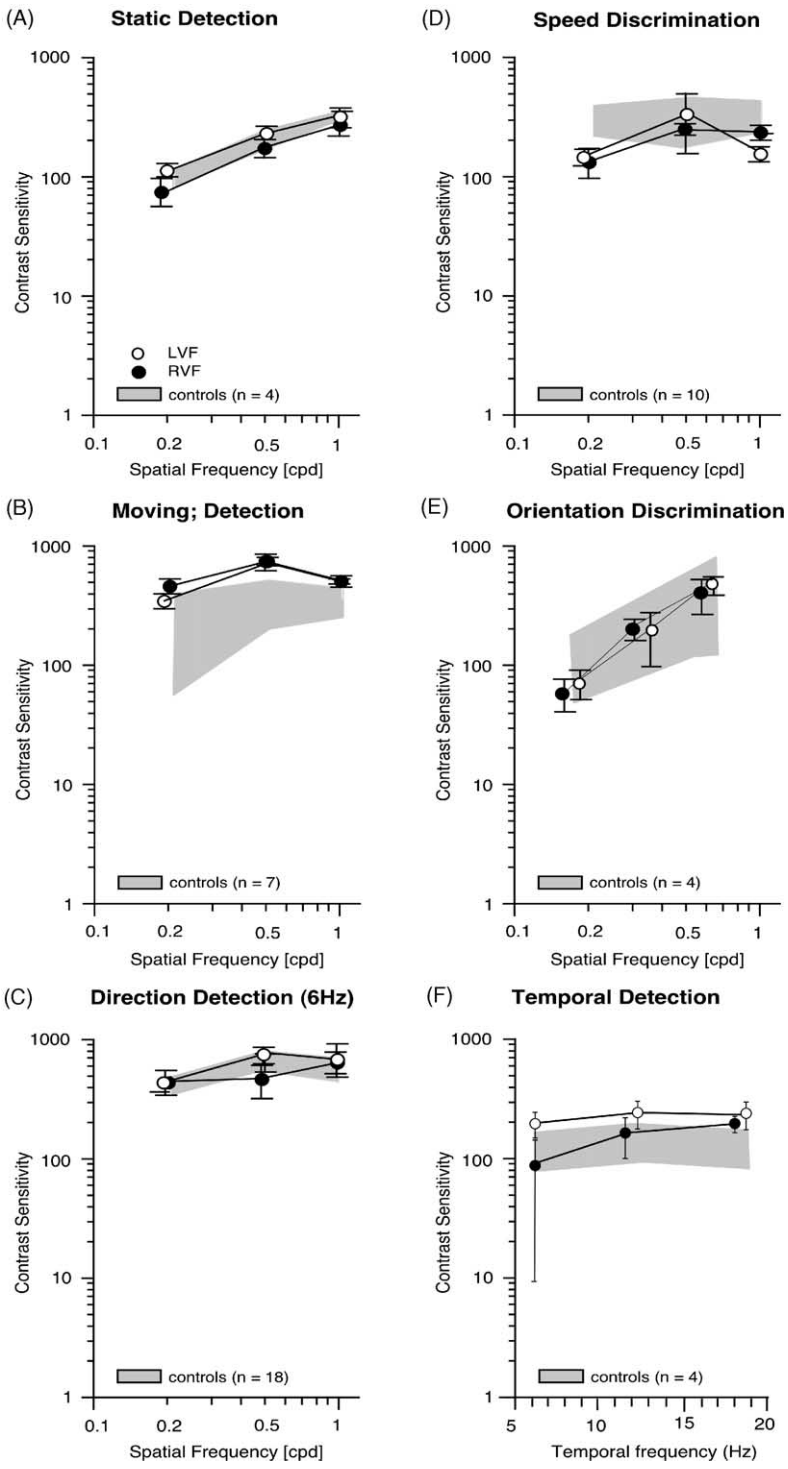

Fig. 2. Contrast sensitivity, detection and discrimination. Stimuli were sinusoidal gratings of 0.2, 0.5 and 1 cycles/degree moving up or down in the middle of the display screen while subjects fixated 2° to the left or right of the lateral borders at midlevel. All tasks were 2TAFC. With the moving stimuli, the standard temporal frequency was 6 Hz. In the orientation discrimination (E) two successive sequences of different orientations (3 and 5°) were presented in random order. The subject was asked to select the smaller angle. The shaded area represents the data from age-matched control subjects (thresholds ± 1S.D.). The performance for stimulus presentation in the right and left visual field was not statistically significantly different and therefore the data were pooled. AMG's performance is shown for her left and right visual field separately.

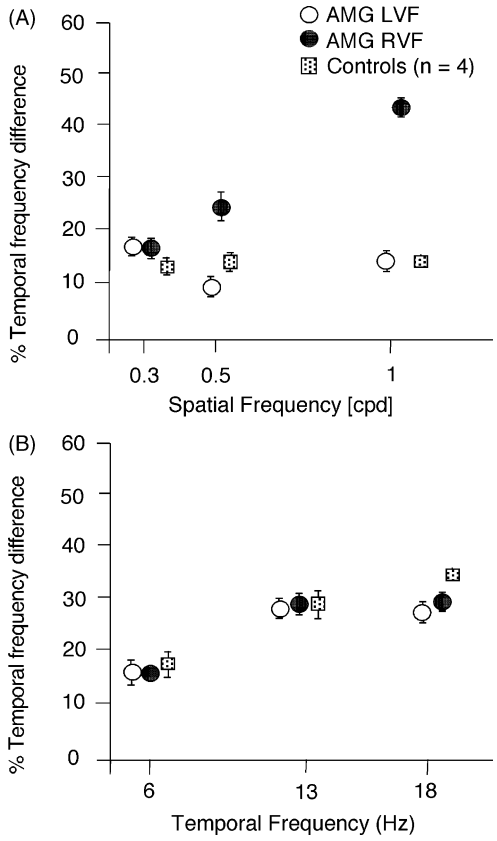

Fig. 3. Counterphase flicker. (A) The stimulus consists of two identical gratings (spatial frequencies 0.3, 0.5 or 1 cycles/degree) superimposed and moving in orthogonal directions at 20°/s. The temporal frequency varied between 3.6 and 6 Hz, 6 and 10 Hz, 10 and 12 Hz, and 18 and 20 Hz. (B) The gratings were fixed in temporal frequency (6, 13, 18 Hz) and slightly varied in spatial frequency. The graphs show discrimination threshold as the percent temporal frequency difference at each spatial frequency necessary for discrimination at 80% correct.

computation, it was important to determine whether she was impaired on other local motion tasks. In the first experiment, we measured D-Max, i.e. the maximum displacement of positional shift of the dots that can sustain a percept of a coherently moving array of dots. In the second test, she performed a local speed discrimination task in a random display. The last experiment in this section, addresses whether random modulations of spatial or temporal frequency affect AMG's ability to discriminate speed.

3. Experiment 1: D-Max

This test measures D-Max in a variant of Braddick's original test (Braddick, 1974). The display consisted of a dense random-dot array viewed through a square aperture subtending 10° × 10° (Fig. 6A). Dot size was 4 arcmin × 4 arcmin. The stimulus consisted of two frames. The dots in the first frame were displaced a distance D (a multiple of 2 arcmin). Each frame was displayed for 500 ms and the inter-frame interval was zero. Between trials the screen was blank at the mean luminance of the target. Contrast was roughly 60%. Using the adaptive staircase procedure the magnitude of the displacement increased until the observer could no longer perceive coherent direction of motion in a specific direction. In a four-alternatives forced-choice task the observer indicated whether the display moved right, left, up or down.

3.1. Results

Fig. 6B shows the data on this task for stimulus presentation in the right and left visual field. The threshold of the control subjects for stimuli presented in either visual field and for the left visual field for AMG was about 40 arcmin. In contrast, AMG's D-Max for stimuli presented in the right visual field, contralateral to her left hemisphere lesion, was about 20 arcmin, showing that she was impaired.

4. Experiment 2: local speed discrimination in dynamic random-dot displays

This test evaluated the perception of the relative speed of two simultaneously presented dynamic random-dot kinematograms. The stimulus consisted of dynamic random-dot kinematograms displayed in two oblong apertures each subtending 5° × 10°, arranged one above the other in the center of the monitor (Fig. 6C). The distance between their centers was 6°. Each aperture contained 50 computer-generated dots. The speeds of the dots, defined as a function of the distance a dot was displaced between successive frames, was uniform within an aperture and was assigned independently for each aperture. The speed of the dots in one aperture (top or bottom at random), the standard, was fixed at 3°/s. The speed of the dots in the other aperture was initially 6°/s and was systematically varied (up or down) by the staircase procedure. In any single trial each dot took a two-dimensional random-walk of constant step size defined by the speed. The direction in which any dot moved was randomly extracted from a 360° range and was independent of its previous direction and also of the displacements of the other dots. (The resolution of the Apple monitor constrained the direction sampling to every 45°.) In a 2AFC task subjects had to indicate in which aperture the dots appeared to move faster.

4.1. Results

Fig. 6D shows the results for stimuli presented in the right and left visual fields, from AMG and eight age-matched normal observers. The data are plotted as threshold of speed difference required for 75% correct performance. The data points for AMG are the average of three threshold estimates obtained in three different sessions several days apart. The Weber fraction for reliable speed discrimination for both the normal controls and AMG in her left visual field, was roughly 0.3. But in her right field her Weber fraction was roughly 0.75, which indicates a substantial impairment.

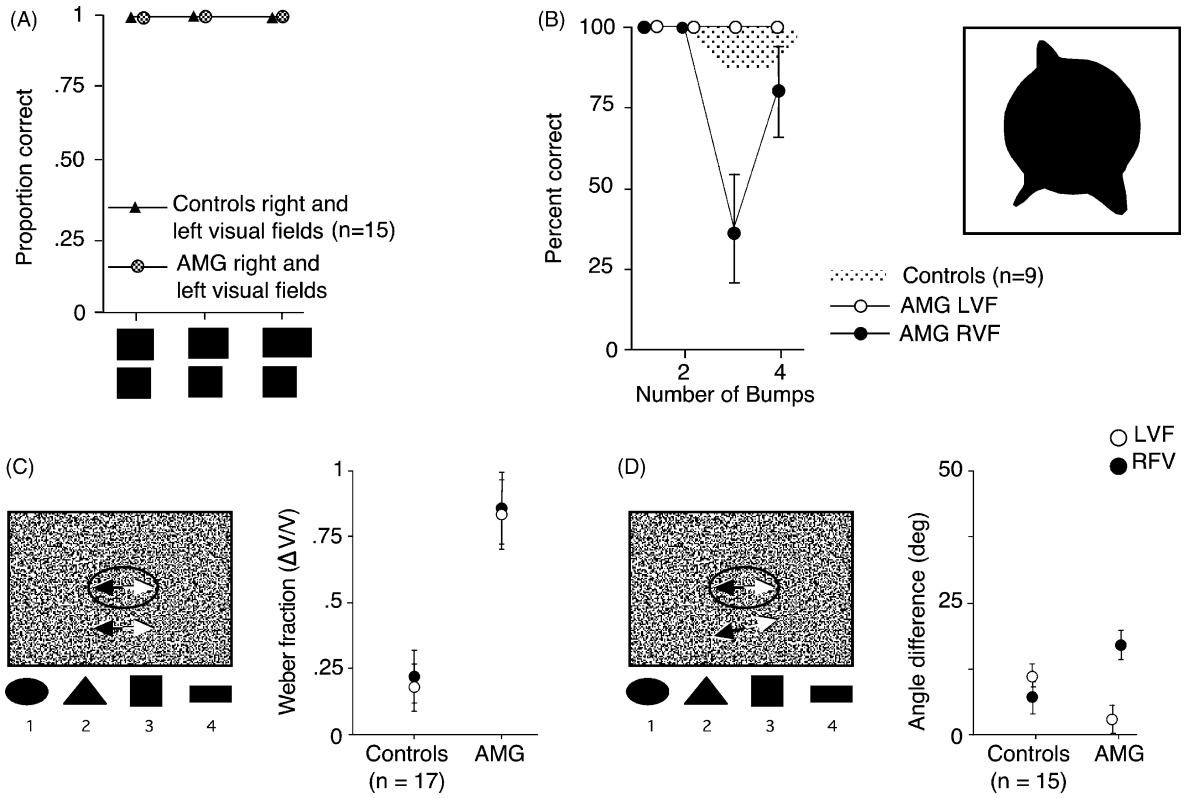

Fig. 4. Diagnostic psychophysical tests: shape, spatial discrimination, 2D form from speed or direction differences. (A) Efron shapes: the performance of AMG is indicated by circles. As there were no differences between performance in the left and right hemifields in either AMG or the normal controls the results have been combined; (B) the stimulus is illustrated on the right. It consists of a circle with one, two, three or four Gaussian bumps added to its circumference at random locations. On each trial two stimuli are presented, one after the other, and in one of the stimuli one of the bumps may be displaced around the circumference. The subject has to decide whether the two stimuli are the same or not. The plot in B illustrates the performance of AMG and nine age-matched control subjects. The shaded area shows the performance of the controls, mean ± 1S.D. Open and filled circles indicate AMG's results for her left and right hemifields, respectively. (C and D) 2D form defined by difference in only speed (C) or direction (D) from the background. On the left is a schematic representation of the stimulus. A contiguous central patch of the dense random-dots pattern moves with a different speed or direction from that of the identically dense background RDK. The patch has one of the four possible shapes, shown below the display. The subject's task is to determine in a 4AFC task the shape of the moving patch. When the patch moves with the same speed and direction as the background, the whole display is uniformly moving left or right. The base speed is 3°/s. The graphs from seven age-matched normal controls and AMG show the results for the stimulus presentation in the left and right visual field when the shape differs from the background only in speed. In (D) the results are shown from five age-matched control subjects and AMG when the shape is defined only by direction difference.

5. Experiment 3: speed discrimination by varying either temporal or spatial frequency

This test addresses the subject's ability to discriminate speed of motion of drifting sinusoidal gratings, as a function of spatial or temporal frequency. The stimuli were horizontally oriented sinusoidal gratings drifting vertically on the oscilloscope's CRT. The presentation order of the standard and variable was randomized from trial to trial in a 2AFC paradigm. The speed of the standard grating was always 20°/s. The speed of the variable grating was always lower than that of the standard and depended on the previous response of the subject in accordance with the adaptive staircase procedure. Because speed is equal to temporal frequency divided by spatial frequency (SF), we generated the speed ranges for the variable-stimulus by either fixing TF and randomly varying SF in a given range, or by fixing SF and randomly varying TF in a given range. For fixed spatial frequency, at 0.3 cycles/degree, the temporal frequency varied between 3.6 and 6 Hz, and at 0.7 cycles/degree, temporal frequency varied between 10 and 14 Hz. For fixed temporal frequency, at 6 Hz the spatial frequency varied between 0.3 and 0.48 cycles/degree and at 13 Hz, spatial frequency varied between 0.65 and 1.04 cycles/degree (Fig. 7).

The observer was asked to determine which stimulus, the first or the second, moved faster. The stimuli were displayed for 500 ms followed by a 500 ms blank screen at the mean luminance of 30 cd/m^2. To eliminate the possible cue of reduced apparent contrast at different spatial frequencies the contrast of the stimuli was randomly varied from trial to trial in the range of 20–30%, which was well above the subject's threshold. To prevent the possibility of judging the speed by the distance traversed by the target on each trial, the duration of the stimuli was randomly varied by ±20% (McKee, Silverman, & Nakayama, 1986).

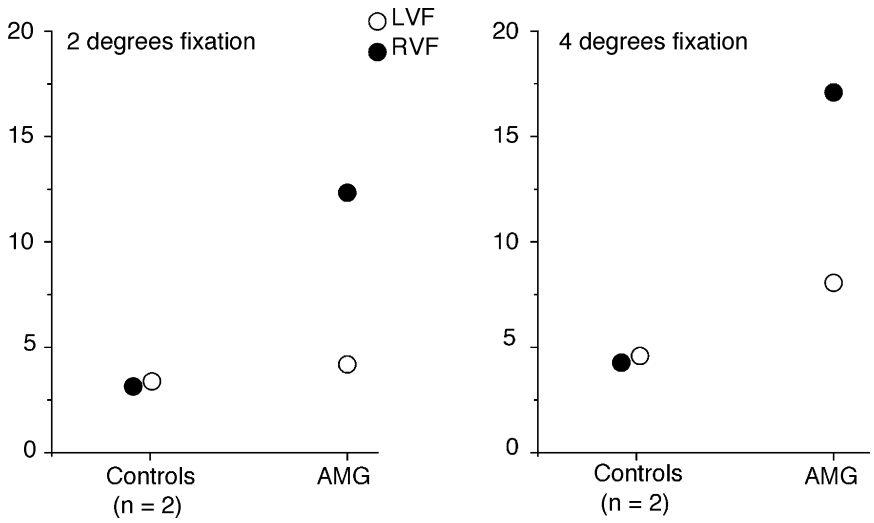

Fig. 5. Stereopsis. The results on the stereotest for AMG and two age-matched controls when the left and right fixations were, left, 2° from the stimulus (shown at the center of the screen) or, right, 4° from the stimulus.

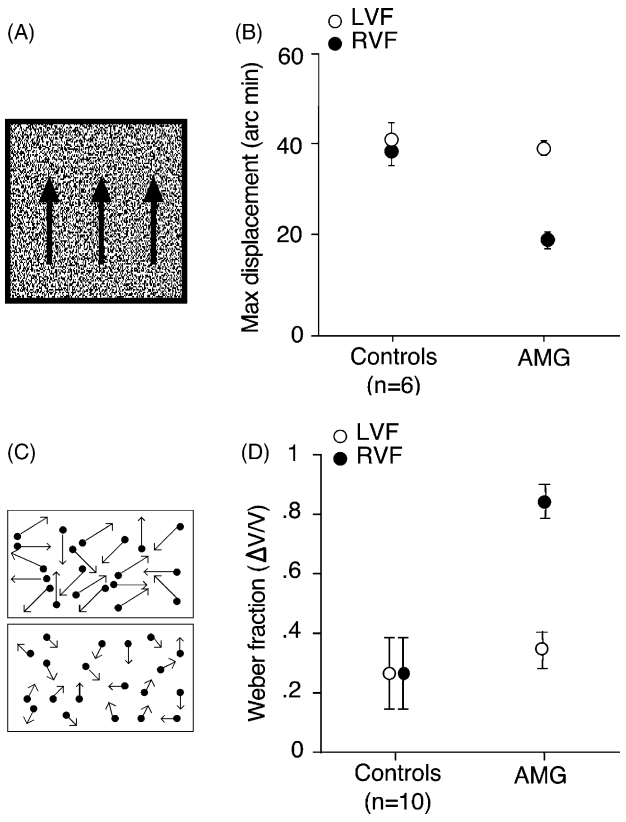

Fig. 6. Local Motion. On the left of each pair of boxes are schematic views of the displays used to test AMG's local motion vision (A: D-Max; C: local speed discrimination). On the right (B and D) are the results for AMG and age-matched normal controls separately for stimuli presented in the right and left visual field. Details are provided in the text.

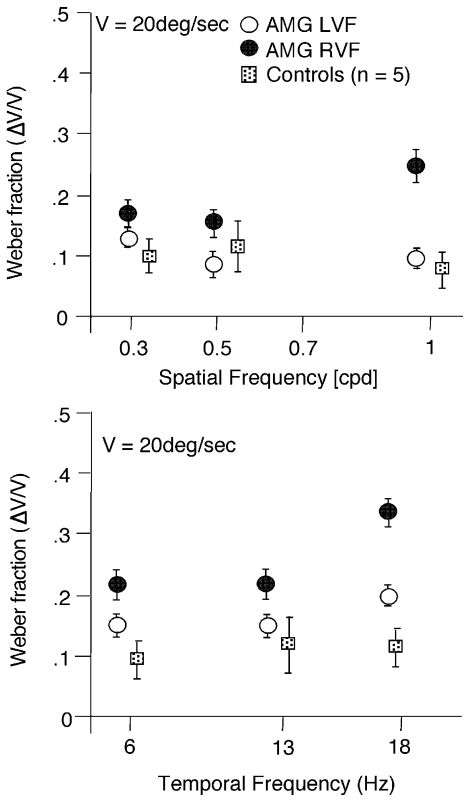

Fig. 7. Speed discrimination: temporal or spatial frequency. The stimuli consisted of vertical sinusoidal gratings which moved horizontally. The direction of motion varied from trial to trial. The standard velocity of the stimulus was 20°/s. Top: Results for stimuli varying in temporal frequency, for fixed spatial frequencies of 0.3, 0.5 and 1 cycles/degree. The stimuli were presented in the right and left visual field. Since there was no statistically significant difference between left and right hemifield presentation in age-matched normal subjects ($n = 5$) the results were pooled. Bottom: Results on speed discrimination task (20°/s for base speed) for AMG and five normal controls for temporal frequencies of 6, 13, and 18 Hz.

5.1. Results

Fig. 7 shows the Weber fraction for velocity discrimination as a function of velocity of sinusoidal gratings of different spatial frequencies (top) or different temporal frequencies (bottom). The control subjects age-matched to AMG had somewhat higher thresholds than the young normals, but the difference was not statistically significant ($t = 1.52$, $P < 0.2$). For stimuli presented in the left visual field, AMG's performance was normal, for all test conditions. However, for stimuli presented in the right visual field, she was impaired, especially on temporal frequencies in the range of 13 Hz ($t = 2.87$, $P < 0.01$). Her performance was normal for either field presentation at the lowest spatial frequencies used. Previous findings (McKee, Silverman, & Nakayama, 1986) on a similar test in normal subjects showed that velocity discrimination is much better at lower spatial frequencies.

5.2. Discussion

Patient AMG was impaired in all three experiments for stimuli presented in the right visual field contralateral to her left hemisphere lesion. Her D-Max in the right visual field was smaller by a factor of two than that of normal subjects and D-Max in her left visual field. D-Max is often interpreted as an indicator of the size of the displacement in the early, local, stage of motion processing over which the "motion-correspondence problem" can be solved (Nakayama & Silverman, 1984). AMG's lower D-Max could indicate involvement in her lesion of a visual area with relatively large receptive fields such as MT or V3A. Neurons in MT have been proposed as the neural substrate of D-Max (Mikami, 1991). Damage to neurons of large receptive fields, may be compensated by recruitment of neurons in the same visual area with smaller receptive fields or by recruitment of another visual area. In either case a smaller D-Max would be expected, as observed in AMG.

Speed discrimination was also impaired in AMG, as her Weber fraction in the right visual field was 75% as compared to 30% in normal subjects and her left visual field. Since in each frame the direction of dot movement was extracted randomly from a distribution, temporal recruiting of motion signals was not possible. Therefore, this was a temporally local task. To our knowledge, a spatial integration of speed signals independent of direction has not previously been demonstrated. Even if such integration exists, the data show that AMG does not make use of it. Additional support for a deficit in mechanisms underlying local speed perception is provided in Section 13.

The third experiment addressed the question of whether AMG's speed impairment could be at least partially explained by a deficit in temporal frequency or in spatial frequency, or both. The data in Fig. 7 show that her speed discrimination of moving gratings is impaired when their temporal frequency is around 13 or 18 Hz and that it is also worst at the highest spatial frequency of about 1.0 cycles/degree. Because the speed was fixed at 20°/s, these data by themselves, though suggestive of a temporal frequency impairment, cannot resolve whether the impairment primarily involves temporal or spatial frequencies. We therefore tested this issue by repeating the same experiment (once only) with 10°/s speed. AMG was impaired at temporal frequencies in the range of 10–13 Hz, but was not impaired at spatial frequencies below 0.7 cycles/degree. Overall the data therefore suggest that AMG's deficit in speed discrimination reflects an impairment in temporal rather than spatial mechanisms.

Relevant to her possible temporal frequency deficit is that AMG was impaired on counterphase flicker discrimination at 10 Hz, for stimuli presented in the right visual field. Counterphase flicker is the sum of two sinewave gratings of identical spatial and temporal frequencies drifting in opposite directions (Levinson & Sekuler, 1975). McKee, Silverman, and Nakayama (1986) argued that temporal frequency discrimination in counterphase flicker is performed indirectly through velocity mechanisms. It is therefore not surprising that AMG's deficits in speed discrimination in the range of 10–13 Hz were also accompanied by a deficit in counterphase flicker perception at 10 Hz.

6. Global motion: temporal and spatial integration of motion signals

There is a wealth of evidence that motion processing depends on local spatial and temporal processes. Several studies (Watamaniuk, Sekuler, & Williams, 1989; Watamaniuk & Sekuler, 1992) have suggested that processes of temporal and spatial integration enhance the performance of subjects on motion tasks. In the next set of experiments, we accordingly tested whether motion integration mechanisms can be used to improve motion perception when local mechanisms are impaired, as in the case of AMG. Experiment 4, adapted from Nakayama and Silverman (1984), addresses the temporal integration stage using the same paradigm as in Experiment 1 (D-Max). Experiment 5, motion coherence, was adapted from Newsome and Paré (1986) and addresses the problem of spatial integration in global motion.

7. Experiment 4: temporal recruiting

To investigate the temporal characteristics of the upper displacement limit, D-Max, we modified Experiment 1 by using six successive frames with a pause between successive presentations in which the dots from the previous frame were displaced a distance, D, in the direction of motion of that display. The displacement was always a multiple of 2 arcmin. The first and last frame were displayed for 500 ms. The independent variable was the duration of the intermediate frames (or steps). The following durations of the intermediate patterns were selected: 16, 32, 48, 64, 80, 96, 112

or 128 ms. The inter-frame interval was zero. All the other test parameters were identical to those in the D-Max test. The subject had to indicate whether the overall direction of motion of the array was up, down, left or right.

7.1. Results

Fig. 8B shows the results of the 8 conditions by plotting the total upper limit threshold against total pause duration. As reported elsewhere (Nakayama & Silverman, 1984) the results show that with lengthening pause between frames the two frame D-Max doubles in about 30 ms both for the control subjects and for AMG. Fig. 8B plots the ratio of D-Max increase from the two frames D-Max to the six frames D-Max for different pause durations. It illustrates the dramatic improvement of AMG's D-Max in her impaired right visual field when temporal recruiting becomes possible.

8. Experiment 5: temporal recruiting in speed discrimination

Experiment 2 addressed the observer's ability to make local speed discrimination. Experiment 5 evaluates the same ability when temporal recruiting becomes possible. The stimulus is shown schematically in Fig. 8C. Instead of moving randomly, all the dots now move in the same direction, up, down, left or right, for the whole 22 frames of the display time. In order to minimize possible distance and duration cues for judging the speed of the dots in a

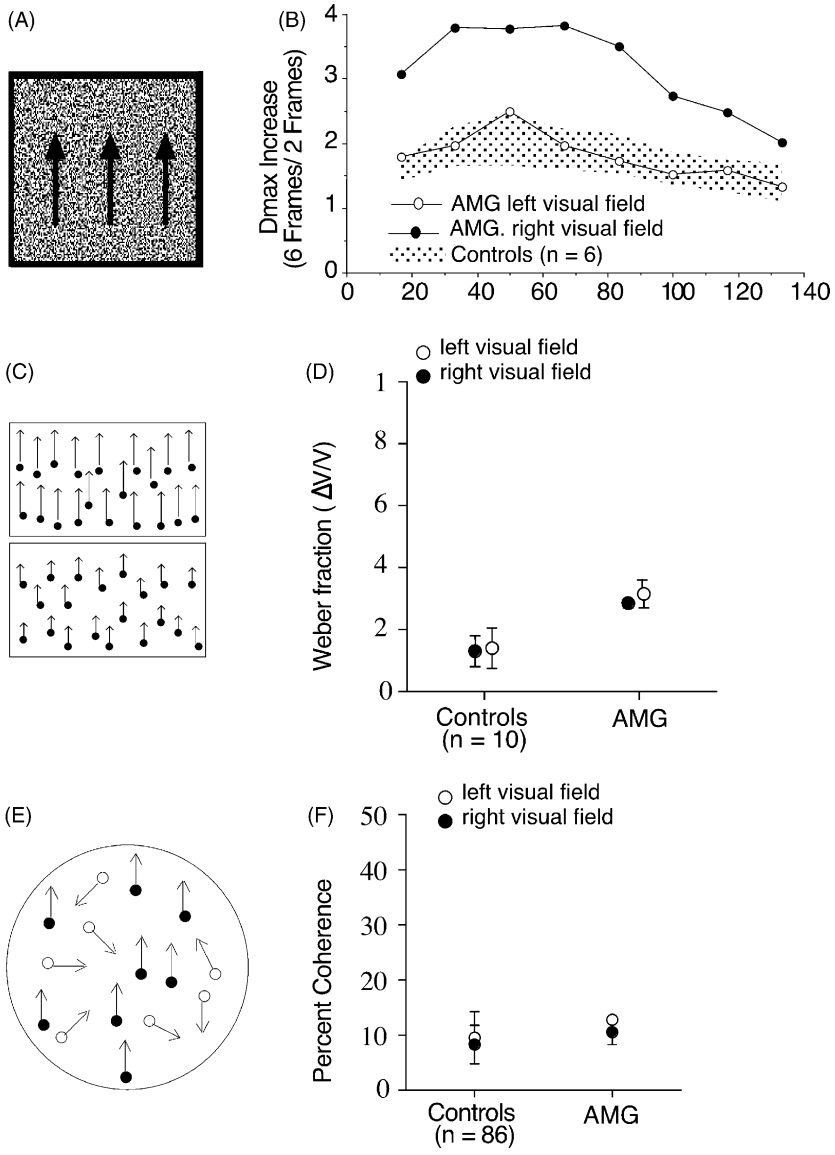

Fig. 8. Motion integration. On the left of each pair of boxes are schematic views of the displays used to test AMG's local motion vision (A: D-Max; C: speed discrimination; D: motion coherence). On the right are the corresponding results from AMG and age-matched normal controls separately for stimuli presented in the right and left visual field. Details are provided in the text.

trial, duration of the stimuli in this test was randomly varied by ±20% (McKee, Silverman, & Nakayama, 1986). Using an adaptive staircase we measured the threshold for the Weber fraction of speed necessary to reliably judge which of the two simultaneously displayed dynamic random-dot cinematograms moved faster.

8.1. Results

Fig. 8D shows the results from AMG and eight age-matched normal subjects. Although AMG performed similarly to the poorest normal control her left and right visual field were now closely matched. Her performance in the right visual field ($\Delta V/V = 28\%$) contrasts sharply with her very impaired performance on the local speed task ($\Delta V/V = 74\%$), (Fig. 6).

9. Experiment 6: motion coherence

The purpose of this experiment was to determine the minimum percentage motion coherence at which a subject could reliably discriminate the direction of coherent motion in a random-dot display. The stimuli, displayed in a $10^\circ \times 10^\circ$ aperture, were dynamic random-dot kinematograms with a correlated motion signal of variable strength embedded in motion noise (a schematic view is shown in Fig. 8E). The strength of the motion signal, that is the percentage of the correlated dots moving in the same direction, varied from 0 to 100%. The uncorrelated dots moved in random directions. At 0% there was no motion signal and at 100% correlation all the dots moved in the same direction. Fig. 8C shows a stimulus with 50% correlation. The algorithm by which the dots were generated was similar to that of Newsome and Paré's (1988) and fully described elsewhere (Vaina, Lemay, Bienfang, Choi, & Nakayama, 1990).

9.1. Results

Fig. 8F shows that AMG was not impaired on this task. Her performance in the right and left fields was almost identical and no different from that of 86 control subjects.[2]

9.2. Discussion

AMG's performance in all three tests of temporal and spatial integration of motion was significantly better than her performance on the local motion tasks. Her six-frame D-Max was normal (Fig. 8B) for presentation in either visual field despite being severely impaired for one instantaneous jump (Fig. 6B). Nakayama and Silverman (1984) suggested two stages with different temporal properties, a fast early stage, which performs the local motion measurement (two-frames D-Max) followed by a slower, integration stage. AMG's normal performance on the six-frame D-Max, especially for inter-frame duration up to about 100 ms, suggests that she uses temporal integration to overcome deficits in local motion measurements and that the local motion stage is not the limiting stage in determining psychophysical performance with moving displays.

In the speed discrimination task where all dots move with the same direction for 22 frames, AMG's performance was normal for stimuli presented in either visual field (Fig. 8D). This contrasts with her severe deficit in the right visual field in the local speed discrimination task (Fig. 6D). This difference cannot be attributed to the subject's use of distance and duration cues, since the duration that a dot spent in the aperture was randomized. We suggest that it arises from AMG's unscathed ability to use temporal (and possibly spatial) recruiting.

In Experiment 5, motion coherence, AMG's performance was normal in both visual fields. This is a task of spatial integration because, to perform it, the subject must pool information over several signal dots to overcome the motion noise. Subjects, including AMG, probably do not use temporal integration in this task, as they can perform it at such low-level of coherence that it is very improbable that any given dot would move in the direction of the signal for more than two frames in a row. Moreover, the direction of the motion field cannot be derived by looking at individual dots, but depends on the integration of motion information over a large area in the display (Downing & Movshon, 1989). In summary, despite AMG's deficits in local motion measurements, her ability to perceive motion stimuli is greatly enhanced by her ability to use mechanisms of spatial and temporal integration of motion signals.

10. Interactions between local and global motion measurements

Adelson and Movshon (1982), Movshon, Addelson, and Gizzi (1983) suggested that for two superimposed sinusoidal gratings moving in different directions to be perceived as a single pattern (plaid) moving rigidly, the visual system must solve the aperture problem. This problem exists because local measurements of motion do not provide sufficient information to indicate unambiguously the motion of two dimensional patterns. They proposed that seeing a plaid move rigidly requires the combination of motion signals over space, although it is possible that the rigid-plaid motion can be computed just by relatively local motion computations and that there is no aperture problem for perceiving

[2] The thresholds of motion coherence obtained by the human observers in the Newsome and Paré's task were roughly 2%. This may be accounted by slight differences in the display characteristics. Dot density in their task was roughly five times higher than in our display (1.7 dot/degree^2 compared with 0.3 dot/degree^2). In addition their subjects were experienced with psychophysical testing and in addition they also received extensive training on the task. Our data (unpublished observation) also suggest the dependency of the threshold of training and psychophysical experience of the observer.

moving plaids. Experiment 7 therefore tests whether the perception of coherence in plaid motion is impaired in AMG, as was the case of all local motion tasks, or whether it is not impaired as was the case with the global motion tasks.

The dichotomy between local and global computations of motion is also relevant to the discussion of the computation of image discontinuities from motion cues. Discontinuities imply a local computation as they involve the existence of an infinite spatial derivative of some visual quantity. Nevertheless, it is possible that although discontinuities and integration are computed separately, they interact. Experiment 8 therefore addresses the ability of normal subjects and AMG to detect discontinuity boundaries in a display where the local motion signal is noisy, as in Experiment 5, and where detecting the discontinuity requires some global computation.

11. Experiment 7: perception of motion transparency

Moving plaid patterns generated by additive superposition of two sine wave gratings were viewed through a circular aperture subtending 8° of visual angle (Fig. 9A). The stimulus was surrounded by a uniform gray field with a luminance equal to the mean luminance of the pattern (22 cd/m^2) and presented for one second. Stimuli were generated by a Macintosh computer and displayed on a Macintosh RGB screen. Two-dimensional spatial patterns were generated by drawing two one-dimensional ramps oriented at 30° on either side of vertical (the IOC direction) into video memory. The appearance of motion was generated by cycling through look-up tables containing sinusoidal values. The two components always had the same contrast of 30%. The spatial frequency of one grating remained fixed at 1 cycles/degree while that of the other was varied between 0.25 and 2.5 cycles/degree in steps of 0.25 cycles/degree. The temporal frequencies of the gratings were chosen to ensure that the speed of each was maintained at 3°/s. Every pattern was repeated 22 times. Observers sat 1 m from the screen in a darkened room, and were instructed to maintain fixation on a spot 6° from the center of the stimulus aperture. All subjects reported that the entire stimulus was in view under these conditions. The experimental task was to indicate whether the moving pattern appeared “coherent” (a plaid) or “transparent” (component stripes sliding over each other).

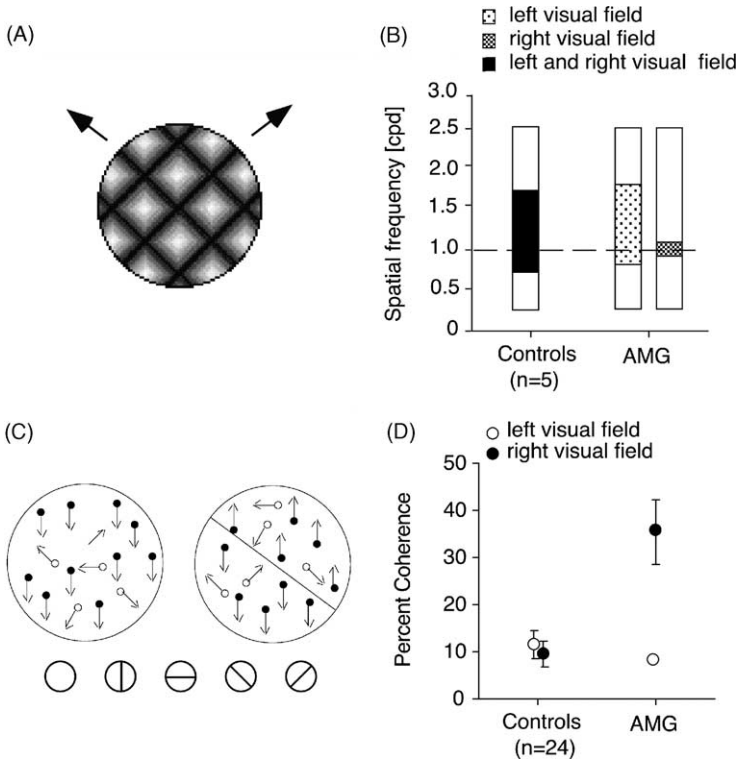

Fig. 9. Plaids and motion discontinuity. (A) Schematic view of the stimulus in the plaid task. The arrows indicate the direction of the component gratings. (B) Coherence/transparency data from AMG and a group of five age-matched normal controls. Subjects had to report whether the pattern appears to be moving coherently (a plaid) or transparently as separate components. The shaded areas represent the range of spatial frequencies of the variable component for which motion was judged coherent on at least 75% of trials. For AMG results for the left and right visual field are shown separately. Normal controls performed similarly in both fields and their data were therefore pooled. (C and D) Motion discontinuity. Schematic illustration of the dynamic random-dot motion display. The motion of the signal dots was always vertical, and in the trials where a motion defined boundary was present the signal directions were opposite. The orientation of the illusory discontinuity line was either horizontal, vertical, or at ±45° of visual angle. (D) The results of AMG and 14 age-matched normal control subjects. The data show performance for the stimulus presented in the left or right visual field.

11.1. Results

Fig. 9B shows that for stimuli presented in the left visual field the normal observers and AMG could detect coherence at ranges between 0.5 and 1.5 cycles/degree. But for stimuli presented in her right visual field, AMG saw the gratings as a coherently moving plaid only when the spatial frequencies of the two gratings were very similar. Adelson and Movshon (1982), Movshon, Addelson, and Gizzi (1983) reported that in normal observers a rigidly moving plaid could be perceived when the two component gratings differed by less than a factor of three in spatial frequency. Because our data were obtained from naive observers and a relatively small number of trials may explain the smaller range of spatial frequencies in which they saw reliably coherent motion.

12. Experiment 8: detection of motion discontinuity

The aim was to determine the threshold motion intensity at which a subject could reliably detect discontinuity from motion cues in dynamic random-dot displays. The display consisted of dynamic random-dots generated as described in Experiment 5 (motion coherence). The major difference was that in roughly half of the trials, at random, an imaginary line divided the display into two parts, defined by the motion of the signal dots in opposite directions. The imaginary line could be placed in one of four possible orientations (Fig. 9C). In the remaining trials the entire field of dots moved homogeneously up or down. The subject had to indicate in a 2AFC procedure whether the imaginary boundary was present in the display but identifying its orientation was not required. As in Experiment 5, on motion coherence, the varying parameter was the systematically altered percentage of signal dots in the display. In order to avoid orientation cues (comparison between direction of motion and border orientation) the dots generated in a $10^\circ \times 10^\circ$ aperture by a method identical to that described in Experiment 5 (motion coherence) were displayed through a circular mask of the same diameter.

12.1. Results

Fig. 9D shows that the normal controls, and AMG for stimuli presented in her left visual field, could perform the task when roughly 10% of the dots moved coherently. However, AMG's performance for stimuli presented in her right visual field was severely impaired (unlike her normal performance on the motion coherence test). She required roughly 40% coherent motion of the dots in order to reliably decide whether the display contained a dividing discontinuity.

12.2. Discussion

In both the transparency and discontinuity tasks, AMG was impaired for stimuli presented in the right visual field but not in the left. She could only perceive rigidly moving plaids when the two component gratings did not differ in spatial frequency by more than a factor of 1.33 in the right visual field. But in the left visual field, like normal subjects, she perceived rigidly moving plaids for spatial frequencies varying up to a factor of 2. One interpretation of her deficit is that she cannot integrate motion information across spatial frequencies. To perceive rigidly moving plaids, even though the direction of each grating is initially detected independently at different spatial frequencies (Adelson & Movshon, 1982; Movshon, Addelson, & Gizzi, 1983; Wilson, Ferrera, & Yo, 1992), normal subjects combine motion information across a range of spatial frequencies. We return to this point in the general discussion.

The results of Experiment 8 show that to detect discontinuities in the right visual field, AMG needed a percentage of signal dots four times higher than that required in her left visual field and by normal subjects. One could interpret this deficit in a similar manner as discussed in the transparency case, namely, as a deficit of integration across spatial scales. Single unit recordings in area V1 have shown that receptive field size decreases monotonically with increase in preferred spatial frequency (Tolhurst & Movshon, 1975). Hence, an impairment in integration across spatial frequencies might imply an impairment in integration across spatial scales. To solve the task in Experiment 8, a subject must combine information across several spatial scales: large scales are necessary to reduce noise, while small scales are necessary to detect the boundary. In view of her normal performance in the motion coherence task (Experiment 5), her spatial integration across large spatial scales appears to be normal. Is it possible that her small-spatial-scale mechanisms are selectively impaired, which would account for her deficits in the discontinuity task? Evidence against this possibility is her normal performance in tasks containing relatively high spatial frequency stimuli.

13. General discussion

The results of the psychophysical tasks suggest that for stimuli presented in the right visual field contralateral to her cerebral lesion, AMG is impaired at low-level encoding of motion information (Experiment 1: D-Max), on the perception of relative speed in a local speed discrimination task (Experiment 2: local speed discrimination), and at moderately high temporal frequency in the range of 10–13 Hz (Experiment 3: speed discrimination by varying either temporal or spatial frequency). In contrast, on the global motion tasks, AMG's performance was normal for tasks involving both temporal (Experiment 4: temporal recruiting) and spatial integration (Experiment 5: motion coherence). However, she was impaired on the discrimination of global speed when carrying out the task that also involved the segregation of two sheets of dots

based on local speed information (Experiment 4: condition B). This pattern of deficits suggested that she was specifically impaired in local motion computations but not on global motion and this was addressed by studying possible interactions between local and global motion computations (Experiment 7: motion transparency; and Experiment 8: motion discontinuity). She was selectively impaired on the tasks probing the integrity of these interactions for stimuli presented on the right visual field. We suggest that this impairment may be due to impaired ability to integrate motion information across different spatial scales.

13.1. A reinterpretation of deficits of local motion processing

AMG's apparent difficulty in integrating motion information across spatial scales provides a new framework to think about her deficits on local motion tasks. It has been proposed that the computation of local velocity involves the combination of information from several directionally selective neurons tuned to different spatial and temporal frequencies (Heeger, Simoncelli, & Movshon, 1996; Snowden, 1994). In this context, impairment of integration across spatial scales would necessarily impair local direction and speed discrimination. The proposal also explains AMG's deficits on D-Max, since the latter is a signature of the maximal spatial displacement for motion measurement and therefore of the range of relative speeds that can be discriminated (Braddick, 1974; Braddick, 1980). Further support for this explanation comes from AMG's performance on an earlier version of the local speed discrimination task (see Vaina, Lemay, Bienfang, & Choi, Nakayama, 1990; Vaina, Grzywacz, & LeMay, 1990). The major difference between the earlier task and Experiment 2 was that we used constant stimuli, instead of a staircase procedure. The standard speed was, as in Experiment 2, 3°/s and the test speeds were 2, 3, or 5°/s greater. In this earlier task, for stimuli in the right visual field, AMG could paradoxically not discriminate speed ratios of 3 and 5, but could discriminate a speed ratio of 2 when the standard was 3°/s. These ratios correspond to local jumps of the dots in the display of about 43, 26, and 17 arcmin for the ratios of 5, 3 and 2, respectively. Because her D-Max in the right visual field was 19 arcmin, it is likely that she could not even "see" motion at the high ratios. The D-Max of normal subjects and AMG's left visual field was about 40 arcmin, which allows good performance at the high speed ratios. A D-Max of 40 arcmin, which is larger than the Braddick limit of 15 arcmin, is consistent with the eccentric presentation of the stimulus (Baker & Braddick, 1982).

In summary, it is now possible to interpret all of AMG's deficits on the local motion tasks described in this paper in terms of her difficulty in integrating across spatial scales and an impairment in mechanisms tuned to relatively high (10–13 Hz) temporal frequencies.

13.2. Possible functional anatomical correlates of the motion deficits

AMG's motion deficits are consistent with anatomical and physiological properties of the cortical motion pathway in macaque monkeys (Maunsell & Van Essen, 1983; Maunsell & Newsome, 1987; Van Essen & Gallant, 1994). This pathway involves visual cortical areas V1, V2, MT, and MST (Maunsell & Newsome, 1987; Andersen, 1997; Merigan & Maunsell, 1993). There is abundant evidence that neurons in area MT are broadly tuned for directions and speeds of motion, and that some of them respond to the motion of moving plaids rather than to the motion of the component gratings (Albright, 1993; Albright & Stoner, 1995; Stoner & Thomas, 1992; Stoner, Albright, & Ramachandran, 1990). Furthermore, damage to area MT impairs motion processing and microstimulation of MT influences perceived direction (for reviews Newsome, Britten, Salzman, & Movshon, 1990; Newsome, Britten, & Movshon, 1989; Salzman, Britten, & Newsome, 1990). Area MT receives its direct input from the striate cortex (V1), and the rest indirectly from V1 via areas V2 and V3. AMG's lesion (Fig. 1) is predominantly lateral occipital. It includes at least part of area 18 and therefore possibly parts of V2 and V3 but it does not include either V1, which occupies the calcarine sulcus and is medial to the lesion, or area MT, which lies ventral to the most ventral extent of her lesion.

To determine more accurately which of these visual areas were involved in the cortical portion of AMG's lesion a second MRI was obtained (Vaina, Gryzwacz, Lemay, & Bienfang, 1994) using a protocol suitable for morphometric three-dimensional reconstruction of the brain. Saggital T1-weighted and axial balanced and T2 spin echo images of the brain were obtained without intravenous contrast. The T2-weighted structural volumes were used to delineate the lesion by registering them in Talairch space. The coordinates and the extent (number of voxels) of the lesion for each slice (Fig. 10) were obtained and a 3D template of the lesion area was created. For lesion localization, region of interest (ROI) analysis and visualization, we used MEDx 3.41 software (Sensor Systems, Sterling, VA).

Guided by published data from functional magnetic resonance imaging studies (Sunaert, Van Hecke, Marchal, & Orban, 1999; Sunaert, 2001; Van Oostende, Sunaert, Van Hecke, Marchal, & Orban, 1997; Mendola, 1999; Tootell et al., 1997; Vaina, Solomon, Chowdhury, Sinha, & Belliveau, 2001; Culham, 2001) we defined several brain ROI known to be involved in the processing of different aspects of visual-motion. Guided by the Talairach coordinates of the motion responsive areas reported in the above publications, we defined templates for ROIs corresponding to areas V1, V2, V3,Vp, V3A, V4, MT, KO and STS. This allowed us compare AMG's lesion with functionally defined areas. After defining the above ROIs, we overlaid them on the structural MRI image of AMG. The result shows that the cortical lesion in AMG is centered on areas V3A and

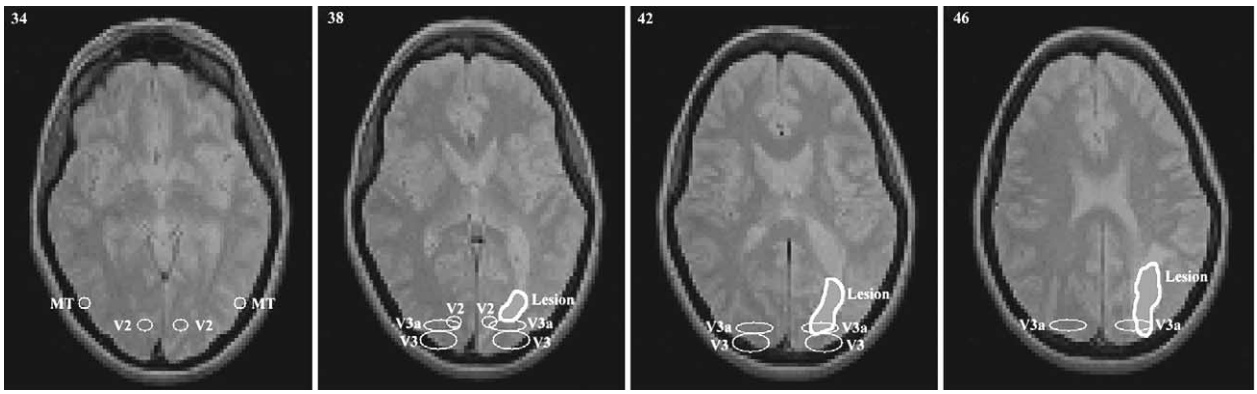

Fig. 10. Lesion localization relative to area MT and to retinotopic areas, shown on axial slices of AMG's brain.

V3 in the left hemisphere, but areas V1, V2, VP, V4, MT, KO, and STS are probably not involved, or at least not directly. This is especially true for areas V1, VP, V4, MT, and STS, since these areas are further away from the lesion. Fig. 10 illustrates how the cortical part of the lesion overlaps with the anatomical templates for areas V3A and V3, but not with V2 and MT. However, like most cerebral lesions, AMG's includes white matter and connections between MT and V1/V2 or V3/V3A may have been damaged. However, our data indicate that if area MT is indirectly damaged the damage is incomplete as AMG can perform the motion coherence task well. There is abundant evidence showing that area MT mediates the perception of global motion associated with that task (Newsome & Paré, 1986; Newsome & Wurtz, 1988; Newsome, Britten, Salzman, & Movshon, 1990; Snowden, Treue, Erickson, & Andersen, 1991; Newsome, Britten, & Movshon, 1989; Salzman, Britten, & Newsome, 1990; Newsome & Paré, 1988; Maunsell & Newsome, 1987).

13.3. The relation of AMG's deficit to models of global spatial and temporal integration

The data in Fig. 8B support the hypothesis of Nakayama and Silverman (1984) that temporal recruiting involves a nonlinear potentiation process, which they suggest might be mediated by neurons in area MT, an area spared in patient AMG. They made their suggestion because two successive displacements provide more information about a moving stimulus, than two independent observations, and because D-Max is reduced at large inter-frame intervals. For a six-frame stimulus presentation in the right visual field, AMG's net increase in D-Max was larger than that of normal subjects, enabling her to reach almost normal performance. Hence, the potentiation of motion information was even larger in her case than in normals. Moreover, at pause intervals larger than 80 ms, her decrease in performance was faster than that of normal subjects, suggesting that the same nonlinear process that cause her steeper potentiation is also responsible for a steeper decline.

A model of temporal integration of motion signals (Grzywacz, Smith, & Yuille, 1989) provides a theoretical framework to account for nonlinear recruiting, and for AMG's ability to reach normal performance with recruiting in spite of local deficits. In its simplest version the model postulates that a global integration stage receives inputs from local velocity vectors and computes a new velocity field even in regions where no local estimate of motion have been made. More recent treatments of the temporal coherence model consider recruiting as a form of Kalman filtering. These treatments are more general than the one presented here, but also much more detailed. We thus prefer in this paper to present the simpler model for its ease of explanation. This velocity field, respects as much as possible the local velocity inputs and simultaneously is spatially and temporally smooth (or coherent). Temporal coherence in this model means that the direction of local motion varies as little as possible over time. Mathematically, this model can be expressed as the minimization of an energy function E over all possible values of the computed velocity field $\boldsymbol{v}(\boldsymbol{r})$ for all positions $\boldsymbol{r}$, and motion-correspondence V_{ia} ($V_{ia} = 0$ or 1 and $\Sigma_{ia} V_{ia} = n$, where n is the number of dots) between dot i in one frame and dot a in the next frame as follows:

$$E(\boldsymbol{v}(\boldsymbol{r}), V_{ia}) = \Psi_1 \sum_{i,a} (\boldsymbol{v}(\boldsymbol{r}_i) - \boldsymbol{U}_i)^2 + \Psi_2 \sum_{i,a} \left(\boldsymbol{v}(\boldsymbol{r}_i) - \frac{r_a - r_i}{\Delta t} \right)^2 + \lambda \int \sum_{m=0}^{\infty} c_m (\nabla^m \boldsymbol{v})^2 \, \mathrm{d}\boldsymbol{r} + \kappa \int \left(\frac{\mathrm{d}}{\mathrm{d}t} \left(\frac{\boldsymbol{v}}{|\boldsymbol{v}|} \right) \right) \mathrm{d}\boldsymbol{r} \quad (1)$$

where $\boldsymbol{U}_i$ is the local velocity input for dot i, $\boldsymbol{r}_a$ and $\boldsymbol{r}_i$ are the positions of dots a and i in the second and first frames, respectively, Δt the pause duration, ∇ the gradient operator, and Ψ_1, Ψ_2, λ, c_m, and κ are positive (except possibly for some c_m) constant parameters. Minimization of the first term in the right hand side of the equation forces the constructed velocity to be similar to the local velocity inputs. Minimization of the second term forces the velocity attributed to the correspondence between dots a and i in consecutive frames

to be similar to the constructed velocity field. Minimization of the third term forces the constructed velocity field to be smooth as it minimizes its spatial derivatives (see Yuille & Grzywacz, 1988, 1989) for a choice of the c_m in which the smoothing is based on Gaussian radial basis functions). Minimization of the fourth term forces temporal variations of direction of motion in the constructed velocity field to be small. Note that the theory justifies minimizing temporal variations of direction instead of speed because for general three-dimensional motions the direction but not the speed of optical flow is invariant.

To understand the implications of temporal coherence, Grzywacz, Smith, & Yuille (1989) simplified Eq. (1) by assuming perfect correspondence for past motion and neglecting spatial coherence effects. In this case, Eq. (1) becomes:

$$E(V_{ia}) = \sum_{i,a} V_{ia}(d_{ia} + \kappa(1 - \cos\theta_{ia})) \quad (2)$$

where d_{ia} is the distance between point i in one frame and point a in the next frame, and θ_{ia} is the angle between the past motion and the direction linking points i and a. To grasp the meaning of this equation, by setting $\kappa = 0$, one eliminates temporal coherence and the model tries to find motions consistent with the smallest overall displacement from frame to frame, exactly as in minimal mapping theory. If $k \neq 0$, then the computed motion would prefer to make $_{ia} = 0$ to minimize Eq. (2). This means that the computed motion would tend to be similar to the past motion.

This temporal-coherence model provides a framework for understanding both the nonlinear potentiation mechanism of temporal recruiting (Nakayama & Silverman, 1984) and AMG's normal performance after recruiting. The potentiation arises because after the past motion signal has built up, the visual system will limit its search for a solution of the motion-correspondence problem predominantly along lines parallel to the direction of past motion. This will decrease the number of false matches in a protocol like that in Experiment 4 and therefore increase D-Max. If one interprets the deficits of AMG as an impairment of local velocity inputs (the first term of the right hand side of Eq. (1)), for example as an imprecise or reduced number of inputs, then the temporal coherence in this model (the fourth term in the right hand side of Eq. (1)) could still raise the D-Max to a normal level. This would occur because pooling the past motion over time minimizes its noise level (that is, would minimize errors in the estimation of V_{ia} in Eq. (2)) allowing for a normal correspondence process (that is, finding V_{ia} in Eq. (2)).

Temporal recruiting also helped AMG in speed discrimination tasks even for stimuli confined to her right visual field. It is puzzling, however, that her best performance and that of normal subjects yielded a Weber fraction of about 0.3 in the speed discrimination tasks of Experiment 2. This contrasts with Weber fractions of about 0.05 in speed discrimination obtained with a wide variety of stimuli (McKee, 1981; McKee, Silverman, & Nakayama, 1986; Orban, De Wolf, & Maes, 1984; McKee & Welch, 1989). The explanation for this discrepancy is not that the computation of global motion involved in spatially wide random-dot displays inhibits the local speed estimates, because one can obtain the 5% value with very dense random-dot kinematograms (Orban, De Wolf, & Maes, 1984). Furthermore, the spatial layout of our stimuli, involving simultaneous stimulation of the upper and lower visual fields is not responsible for a large Weber fraction for speed (Stone & Thompson, 1992; Thompson, 1982, 1990; Thompson, Stone, & Swash, 1996; Verghese & Stone, 1996). However, it is possible that the relatively small number of trials and the absence of training of naive subjects elevated the Weber fraction. Additionally, the low density of dots in our kinematograms, as compared with other speed discrimination studies (Orban, De Wolf, & Maes, 1984), resulted in a lower motion energy signal at low spatial frequencies. The Fourier components of the dots at low frequencies have relatively constant phase from dot to dot and therefore they add over all dots. For a dense RDK, there are more dots and thus the amplitude of the moving low-frequency components is higher.

Acknowledgements

This research was supported by the National Institutes of Health Grant 2RO1 EY-07891 to LMV, and by an MRC grant and an Oxford McDonnell-Pew Network grant to AC.

References

Adelson, E. H., & Bergen, J. R. (1985). Spatio-temporal energy models for the perception of motion. *Journal of Optical Society of America A, 2*, 284–299.

Adelson, E. H., & Movshon, J. A. (1982). Phenomenal coherence of moving visual patterns. *Nature, 300*, 523–525.

Albright, T. D. (1993). Cortical processing of visual motion. In F. A. Miles & J. Wallman (Eds.), *Visual motion and its role in the stabilization of gaze* (pp. 177–201). New York: Elsevier.

Albright, T., & Stoner, G. (1995). Visual motion perception. *Proceedings of the National Academy of Sciences U.S.A., 92*, 2433–2440.

Andersen, R. A. (1997). Neural mechanisms of visual motion perception in primates. *Neuron, 18*, 865–872.

Anstis, S. M., & Ramachandran, V. (1987). Visual inertia in apparent motion. *Vision Research, 27*, 755–764.

Baker, C. L., & Braddick, O. (1982). The basis of area and dot number effects in random dot motion perception. *Vision Research, 22*, 1253–1259.

Baker, C. L. J., Hess, R. F., & Zihl, J. (1990). The "motion-blind" patient: Perception of random dot "limited-lifetime" motion. *Investigative Opthalmology and Visual Science, 31*, 1178.

Braddick, O. (1974). A short-range process in apparent motion. *Vision Research, 14*, 519–527.

Braddick, O. J. (1980). Low-level and high-level processes in apparent motion. *Philosophical Transactions of the Royal Society B, 290*, 137–151.

Braddick, O. (1993). Segmentation versus integration in visual motion processing. *Trends in Neurosciences, 16*, 263–268.

Bravo, M., & Watamaniuk, S. (1995). Evidence for two speed signals: A coarse local signal for segregation and a precise global signal for discrimination. *Vision Research, 35*, 89–103.

Britten, K. H. et al., (1993). Responses of neurons in macaque MT to stochastic motion signals. *Visual Neuroscience*, *10*, 157–1169.
Culham, J. C. (2001). Visual motion and the human brain: What has neuroimaging told us? *Acta Psychologica*, *107*, 69–94.
De Bruyn, B., & Orban, G. A. (1988). Human velocity and direction discrimination measured with random dot patterns. *Vision Research*, *28*, 1323–1335.
Downing, C. J., & Movshon, J. A. (1989). Spatial and temporal summation in the detection of motion in stochastic random dot displays. *Investigative Ophthalmology and Visual Science*, *30*, 72.
Ferrera, V. P., & Wilson, H. R. (1990). Perceived direction of moving two-dimensional patterns. *Vision Research*, *30*, 273–288.
Grzywacz, N. M., Smith, J. A., & Yuille, A. L. (1989). A common theoretical framework for visual motion's spatial and temporal coherence. *Workshop on visual motion* (pp. 149–155). CA: Irvine.
Grzywacz, N. M., & Yuille, A. L. (1990). A model for the estimate of local image velocity by cells in the visual cortex. *Proceedings of the Royal Society B*, *239*, 129–161.
Heeger, D. J. (1987). *Computational model of cat striate physiology*. Massachusetts Institute of Technology.
Heeger, D. J., & Simoncelli, E. P. (1992). Model of visual motion sensing. In L. Harris & M. Jenkins (Eds.), *Spatial vision in humans and robots* (pp. 363–392). New York: Cambridge University Press.
Heeger, D. J., Simonceli, E. P., & Movshon, J. A. (1995). Computational models of cortical visual processing. *Proceeding of the National Academy of Sciences U.S.A.*, *93*, 623–627.
Heeger, D. J., Simoncelli, E. P., & Movshon, J. A. (1996). Computational models of cortical visual processing. *Proceedings of the National Academy of Sciences U.S.A.*, *93*, 623–627.
Hildreth, E. C. (1984a). The computation of the velocity field. *Proceedings of the Royal Society London B*, *B221*, 189–220.
Hildreth, E. C. (1984b). *The measurement of visual motion*. Cambridge, MA: MIT Press.
Hildreth, E. C., & Koch, C. (1987). The analysis of visual motion: From computational theory to neuronal mechanisms. *Annual Review of Neuroscience*, *10*, 477–533.
Koch, C., Wang, H. T., & Mathur, B. (1989). Computing motion in the primate's visual system. *Journal of Experimental Biology*, *146*, 115–139.
Levinson, E., & Sekuler, R. (1975). Inhibition and disinhibition of direction-specific mechanisms in human vision. *Nature*, *254*, 692–694.
Marr, D., & Ullman, S. (1981). Directional selectivity and its use in early visual processing. *Proceedings Royal Society London B*, *200*, 269–294.
Maunsell, J. H. R., & Van Essen, D. C. (1983). Functional properties of neurons in middle temporal visual area of the macaque monkey. I. Selectivity for stimulus direction, speed, and orientation. *Journal of Neurophysiology*, *49*, 1127–1147.
Maunsell, J. H. R., & Newsome, W. T. (1987). Visual processing in monkey extrastriate cortex. *Annual Review of Neuroscience*, *10*, 363–401.
McKee, S. P. (1981). A local mechanism for differential velocity detection. *Vision Research*, *21*, 491–500.
McKee, S. P., Silverman, G. H., & Nakayama, K. (1986). Precise velocity discrimination despite random variations in temporal frequency and contrast. *Vision Research*, *26*, 609–619.
McKee, S. P., & Welch, L. (1989). Is there a constancy for velocity? *Vision Research*, *29*, 553–561.
Mendola, J. (1999). The representation of illusory and real contours in human cortical visual areas revealed by functional magnetic resonance imaging. *Journal of Neuroscience*, *19*, 8560–8572.
Merigan, W. H., & Maunsell, J. H. R. (1993). How parallel are the primate visual pathways? *Annual Review of Neuroscience*, *16*, 369–402.
Mikami, A. (1991). Direction selective neurons respond to short-range and long-range apparent motion stimuli in Macaque visual area MT. *International Journal of Neuroscience*, *61*, 101–112.
Mikami, A., Newsome, W. T., & Wurtz, R. H. (1986a). Motion selectivity in Macaque visual cortex. II. Spatiotemporal range of directional interactions in MT and V1. *Journal of Neurophysiology*, *55*, 1328–1339.
Mikami, A., Newsome, W. T., & Wurtz, R. H. (1986b). Motion selectivity in Macaque visual cortex. I. Mechanisms of direction and speed selectivity in extrastriate area MT. *Journal of Neurophysiology*, *55*, 1308–1327.
Movshon, J. A., Addelson, E. H., & Gizzi, M. S. (1983). The analysis of moving visual patterns. *Pontificiae Academia Scientiarum Scripta Varia*, *54*, 117–151.
Movshon, J. A., & Newsome, W. T. (1996). Visual response properties of striate cortical neurons projecting to area MT in macaque monkeys. *Journal of Neuroscience*, *8*, 2201–2211.
Nakayama, K., & Silverman, G. (1984). Temporal and spatial characteristics of the upper displacement limit for motion in random dots. *Vision Research*, *24*, 293–299.
Nawrot, M., & Sekuler, R. (1990). Assimilation and contrast in motion perception: Explorations in cooperativity. *Vision Research*, *30*, 1439–1451.
Newsome, W. T., Britten, K. H., & Movshon, J. A. (1989). Neuronal correlates of a perceptual decision. *Nature*, *341*, 52–54.
Newsome, W. T., Britten, K. H., Salzman, C. D., & Movshon, J. A. (1990). Neuronal mechanisms of motion perception. *Cold Spring Harbour Symposia in Quantitative Biology*, *55*, 697–705.
Newsome, W. T., & Paré, E. B. (1986). MT lesions impair discrimination of direction in a stochastic motion display. *Society for Neuroscience Abstracts*, *12*, 1183.
Newsome, W. T., & Paré, E. B. (1988). A selective impairment of motion perception following lesions of the middle temporal visual area (MT). *Journal of Neuroscience*, *8*, 2201–2211.
Newsome, W. T., & Wurtz, R. H. (1988). Probing visual cortical function with discrete chemical lesions. *Trends in Neuroscience*, *11*, 394–400.
Orban, G., De Wolf, J., & Maes, H. (1984). Factors influencing velocity coding in the human visual system. *Vision Research*, *24*, 33–39.
Pasternak, T. (1987). Discrimination of differences in speed and flicker rate depends on directionally selective mechanisms. *Vision Research*, *27*, 1881–1890.
Reichardt W. (1965). Autocorrelation: a principle for the evaluation of sensory information by the central nervous system. In W. A. Rosenblith (Ed.), *Sensory communication* (pp. 302–317). New York: Wiley.
Reichardt, W. (1987). Evaluation of optical motion information by movement detectors. *Journal of Comparative Physiology A*, *161*, 533–647.
Rodman, H. R., & Albright, T. D. (1989). Single-unit analysis of pattern-motion selective properties in the middle temporal visual area (MT). *Experimental Brain Research*, *75*, 53–64.
Salzman, C. D., Britten, K. H., & Newsome, W. T. (1990). Cortical microstimulation influences perceptual judgements of motion direction. *Nature*, *346*, 174–177.
Sato, T. (1989). Reversed apparent motion with random dot patterns. *Vision Research*, *29*, 1749–1758.
Snowden, R. J. (1994). Motion processing in the primate cerebral cortex. In A. T. Smith & R. J. Snowden (Eds.), *Visual detection of motion*. London: Academic Press.
Snowden, R. J., & Braddick, O. J. (1989). The combination of motion signals over time. *Vision Research*, *29*, 1621–1630.
Snowden, R. J., Treue, S., Erickson, R. G., & Andersen, R. A. (1991). The response of area MT and V1 neurons to transparent motion. *Journal of Neuroscience*, *11*, 2768–2785.
Stone, L. S., & Thompson, P. (1992). Human speed perception is contrast dependent. *Vision Research*, *32*, 1535–1549.
Stoner, G. R., Albright, T. D., & Ramachandran, V. S. (1990). Transparency and coherence in human motion perception. *Nature*, *344*, 153–155.
Stoner, G. R., & Thomas, D. A. (1992). Neural correlates of perceptual motion coherence. *Nature*, *358*, 412–414.
Sunaert, S. (2001). Functional magnetic resonance imaging: Studies of visual motion processing in the human brain. *Acta Biomedica Lovaniensia*, *226*, 1–123.

Sunaert, S., Van Hecke, P., Marchal, G., & Orban, G. A. (1999). Motion-responsive regions of the human brain. *Experimental Brain Research*, *127*, 355–370.

Tanaka, K., Hikosake, K., Saito, H., Yukie, M., Fududa, Y., & Iwaia, E. (1986). Analysis of local and wide-field movements in the superior temporal visual areas of the macaque monkey. *Journal of Neuroscience*, *6*, 134–144.

Thompson, P. (1982). Perceived rate of movement depends on contrast. *Vision Research*, *22*, 377–380.

Thompson, P. (1990). Motion psychophysics. In J. Wallman & F. A. Miles (Eds.), *Visual motion and its role in the stabilization of gaze* (pp. 29–52). Amsterdam: Elsevier.

Thompson, P., Stone, L. S., & Swash, S. (1996). Speed estimates from grating patches are not contrast-normalized. *Vision Research*, *36*, 667–674.

Tolhurst, D. J., & Movshon, J. A. (1975). Spatial and temporal contrast sensitivity of striate cortex neurons. *Nature*, *176*, 87–100.

Tootell, R. B., Mendola, J. D., Hadjikhani, N. K., Ledden, P. J., Liu, A. K., Reppas, J. B., & Sereno, M. I. (1997). Functional analysis of V3A and related areas in human visual cortex. *Journal of Neuroscience*, *17*, 7060–7078.

Vaina, L. M. (1994). Functional segregation of color and motion processing in the human visual cortex: Clinical evidence. *Cerebral Cortex*, *4*, 555–572.

Vaina, L. M. (1998). Complex motion perception and its deficits. *Current Opinion in Neurobiology*, *8*, 494–502.

Vaina, L. M., Grzywacz, N. M., & Kikinis, R. (1994). Segregation of computation underlying perception of motion discontinuity and coherence. *NeuroReport*, *5*, 2289–2294.

Vaina, L. M., Grzywacz, N. M., & LeMay, M. (1990). Structure from motion with impaired local-speed and global motion-field computations. *Neural Computation*, *2*, 420–435.

Vaina, L., Gryzwacz, N. M., LeMay, M., & Bienfang, D. (1994). Selective deficits of motion integration and segregation mechanisms with unilateral extrastriate brain lesions. *Investigative Ophthalomology and Visual Science*, *35*, 1438.

Vaina L. M., Grzywacz, N. M., LeMay, M., Bienfang, D., & Wolpow, E. (1998). Perception of motion discontinuities in patients with selective motion deficits. In T. Watanabe (Ed.), *High level visual motion* (pp. 213–247). Cambridge: MIT Press.

Vaina, L. M., LeMay, M., Bienfang, D. C., Choi, A. Y., & Nakayama, K. (1990). Intact "biological motion" and "structure from motion" perception in a patient with impaired motion mechanisms: A case study. *Visual Neuroscience*, *5*, 353–369.

Vaina, L., Solomon, J., Chowdhury, S., Sinha, P., & Belliveau, J. W. (2001). Functional neuroanatomy of biological motion perception in humans. *Proceedings of the National Academy of Sciences U.S.A.*, *98*, 11656–11661.

Van Essen, D. C., & Gallant, J. L. (1994). Neural mechanisms of form and motion processing in the primate visual system. *Neuron*, *13*, 1–10.

Van Santen, J. P. H., & Sperling, G. (1985). Elaborated Reichardt detectors. *Journal Optical Society of America A*, *2*, 300–321.

Van Oostende, S., Sunaert, S., Van Hecke, P., Marchal, G., & Orban, G. A. (1997). The kinetic occipital (KO) region in man: An fMRI study. *Cerebral Cortex*, *7*, 690–701.

Verghese, P., & Stone, L. S. (1996). Perceived visual speed constrained by image segmentation. *Nature*, *381*, 161–163.

Verghese, P., Watamaniuk, S. N., McKee, S. P., & Grzywacz, N. M. (1999). Local motion detection cannot account for detectability of an extended trajectory in noise. *Vision Research*, *39*, 19–30.

Watamaniuk, S. N., & Duchon, A. (1992). The human visual system averages speed information. *Vision Research*, *32*, 931–941.

Watamaniuk, S. N. J., & Sekuler, R. (1992). Temporal and spatial integration in dynamic random-dot stimuli. *Vision Research*, *32*, 2341–2347.

Watamaniuk, S. N. J., Sekuler, R., & Williams, D. W. (1989). Direction perception in complex dynamic displays: The integration of direction information. *Vision Research*, *29*, 47–59.

Watson, A. B., & Ahumada, A. J. (1985). A model of human visual-motion sensing. *Journal Optical Society of America A*, *2*, 322–342.

Williams D. W., & Brannan J.R. (1994). Visual detection of local motion signals. In A. T. Smith & R. J. Snowden (Eds.), *Visual detection of motion* (pp. 291–305). London: Academic Press.

Wilson, H. R., Ferrera, V. P., & Yo, C. (1992). A psychophysically motivated model for two-dimensional motion perception. *Visual Neuroscience*, *9*, 79–97.

Yo, C., & Wilson, H. R. (1992). Perceived direction of moving two-dimensional patterns depends on duration. *Vision Research*, *32*, 135–147.

Yuille, A. L., & Grzywacz, N. M. (1989). A mathematical analysis of the motion coherence theory. *International Journal of Computational Vision*, *3*, 155–175.

Yuille, A. L., & Grzywacz, N. M. (1988). A computational theory for the perception of coherent visual motion. *Nature*, *333*, 71–74.